Biogeotechnics 4 (2026) 100132

Contents lists available at ScienceDirect

Biogeotechnics

journal homepage: www.keaipublishing.com/en/journals/biogeotechnics/

Technical Note

Mechanical properties and stability of zinc-contaminated red clay cured by MICP synergistically activated MgO

Yu Song[a,b], Wei Liu[a,b,*], Jiaqi Li[a,b], Yuling Chen[a,b], Jichun Cheng[a,b], Jianwei Zhang[c], Junjie Zheng[d]

[a] School of Civil Engineering, Guilin University of Technology, Guilin 541001, China
[b] Key Laboratory of Karst Dynamics, MNR & Guangxi, Institute of Karst Geology, CAGS, Guilin 541004, China
[c] School of Civil Engineering and Architecture, Henan University, Kaifeng 475004, China
[d] School of Civil Engineering, Wuhan University, Wuhan 430072, China

ARTICLE INFO

Keywords:
Microbially induced carbonate precipitation (MICP)
Strength
Curing
Toxicity characteristic leaching procedure

ABSTRACT

Microbially induced carbonate precipitation (MICP) technology offers an innovative approach for the solidification and stabilization of heavy metal-contaminated soils; However, the mechanical strength and long-term stability of this remediation method have not been thoroughly investigated. This study introduces an innovative curing and stabilization technique using MICP-activated MgO to address the geotechnical challenges posed by zinc ion-contaminated soils. To investigate the effect of zinc ions on soil and the optimal efficacy of MICP-activated MgO in curing zinc contamination, experiments were conducted on zinc-contaminated soils with varying zinc ion concentrations (0.05%, 0.1%, 0.5%, 1.0%), dry densities (1.35, 1.4, 1.45, 1.5 g/cm^3), and activated MgO admixtures (1%, 2%, 5%, 10%). The effectiveness of MICP-activated MgO was evaluated through macroscopic analysis and stability tests, including unconfined compressive strength tests, direct shear tests, and the Toxicity Characteristic Leaching Procedure (TCLP). The results indicated that zinc ions disrupted soil particle cementation, enlarged inter-particle pores, and significantly reduced both unconfined compressive strength and shear strength. The optimal dosage of MICP-activated MgO for curing zinc-contaminated soil was determined to be 10%, resulting in an unconfined compressive strength of 1.196 MPa and a Zn^{2+} leaching concentration of 0.1414 mg/L. The combined actions of MICP-activated MgO facilitated the formation of alkaline magnesium carbonate, calcium carbonate, and magnesium hydroxide. These compounds filled the inter-particle pores of zinc-contaminated soil, encapsulating and co-precipitating zinc ions, thereby enhancing the soil's strength and stability. These findings establish a theoretical foundation for the engineering application of MICP-activated MgO in the remediation of zinc-contaminated soils.

1. Introduction

The rapid development of industry and agriculture in China has resulted in varying degrees of heavy metal contamination in agricultural land. It is estimated that approximately 150 million mu of arable land has been affected, resulting in the annual pollution of around 1.2 billion tonnes of grain (Wang et al., 2003; Teng et al., 2010). The National Soil Pollution Survey reports that overall heavy metal contamination in China's soil exceeds safety standards by 16.1%, with arable land showing a 19.4% exceedance, and industrial and surrounding areas demonstrating a 36.3% exceedance. Consequently, the remediation of heavy metal-contaminated soils is of utmost importance. Currently, the primary remediation methods for heavy metal-contaminated soils include physical remediation technology, chemical remediation technology, and bioremediation technology, among others (Rajendran et al., 2022). Among these, physical remediation techniques are highly efficient but involve high energy consumption and substantial treatment costs (Wang et al., 2021; Xu et al., 2022). Chemical remediation techniques can alter the form of heavy metals; however, they pose risks of secondary hazards and often lead to inadequate stabilization (Xu et al., 2021). Bioremediation technology addresses the shortcomings of other methods, being environmentally friendly, aligning with the national strategic goal of sustainable development, and offering extensive application prospects (Shen et al., 2023; Verma et al., 2021; Xu & Wang, 2023).

* Corresponding author.
E-mail address: 2120220803@glut.edu.cn (W. Liu).

https://doi.org/10.1016/j.bgtech.2024.100132
Received 20 April 2024; Received in revised form 18 July 2024; Accepted 24 July 2024
Available online 2 August 2024

Microbially induced carbonate precipitation (MICP) technology has been proven to effectively remediate heavy metal-contaminated soil. This process primarily involves urease decomposing urea, leading heavy metal ions to react with carbonate and deposit in mineralized forms, thereby fixing them within crystal structures. Additionally, some heavy metal ions are encapsulated by generated calcium carbonate, further immobilizing them within the soil (Torres-Aravena et al., 2018; Warren et al., 2001). Ji et al. (2024) reported that MICP is a highly effective remediation strategy for heavy-metal-contaminated sludge-amended soils. During MICP, the resulting biogenic calcite immobilized Pb, Cd, and Zn by facilitating a shift from highly mobile exchangeable states to stable carbonate-bound and residual forms, leading to a substantial decrease in extractable heavy metal concentrations. In additon, Zha et al. (2024) reported that MICP effectively remediates Pb-contaminated soils. The induced calcium carbonate precipitation fills soil pores and encapsulates Pb^{2+}, thereby significantly improving soil strength and enhancing lead stabilization within the matrix. Dong et al. found that MICP effectively solidified and remediated heavy metals in Pb-Zn tailings, as confirmed by SEM, XRD, FTIR, EDS, and XPS tests. MICP promotes the precipitation of CO_3^{2-} and alkaline substances in the cementing solution, enabling heavy metal ions released from lead and zinc tailings to form stable metal carbonates. This process enhances the structural stability of the tailings. In specimens with a tailing thickness of 2 cm, the unconfined compressive strength reached up to 0.93 MPa after MICP treatment, with a calcium carbonate content of up to 7.41% (Dong et al., 2023). Through MICP technology combined with external dopants for the remediation of contaminated soil and soil reinforcement, it was found that MICP effectively enhances mechanical properties when coupled with external dopants. Calcium carbonate generated internally attaches to soil particles, while external dopants between particles increase adhesion and friction. External dopants also serve as nucleation sites for calcium carbonate formation, thereby significantly enhancing soil strength after consolidation (Hu et al., 2023; Jiang et al., 2022; Li et al., 2022; Wang et al., 2022a; Wang et al., 2025; Shan et al., 2022; Song et al., 2026). Activated MgO is an alkaline and environmentally friendly material characterized by a large specific surface area and strong adsorption capacity, making it an excellent adsorbent. Activated MgO can enhance the mechanical properties of soil and stabilize heavy metal ions, presenting significant prospects in engineering applications (Liu & Li, 2015; Zha et al., 2022). However, there is limited research on the remediation of contaminated soil using MICP combined with external additives, and the impact of additives on the MICP process is also underexplored. Therefore, this study investigates the use of MICP combined with activated MgO for the remediation of zinc-contaminated soil.

In this paper, the mechanical properties and stability of zinc-contaminated soil treated with MICP synergized with activated MgO are investigated experimentally. The study examined the impacts of varying dry densities, different dosages of activated MgO, and different concentrations of Zn^{2+} on red clay with MICP treatment, utilizing unconfined compressive strength tests and direct shear tests. The stability effect of MICP synergized with activated MgO in remediating zinc-contaminated red clay was evaluated using the toxicity characteristic leaching procedure. Finally, the mechanism underlying the synergy between MICP and activated MgO was analyzed, and the process of MICP in conjunction with activated MgO was briefly described. This analysis aims to provide theoretical guidance for the remediation of contaminated soil using MICP combined with activated MgO, facilitating practical applications in engineering.

2. Test materials and methods

2.1. Test material

2.1.1. Microorganisms and reaction fluids

The strain utilized in the experiment was Bartonella sporosarcina pasteurii, and the reaction solution consisted of 1 mol/L $CaCl_2$, 3 g of nutrient broth, and 1 mol/L urea. Bartonella sporosarcina pasteurii needs to be activated after cultivation. The composition of the liquid medium is shown in Table 1. The strain was cultured at a temperature of 30 ˚C with an oscillation frequency of 180 r/min. The bacterial liquid, after 48 h of incubation to reach the stable phase, was selected for the test.

Table 1
Composition of the culture medium.

Name (of a thing)	Culture medium
Yeast extract	20 g
$(NH_4)_2SO_4$	10 g
Tris-base	15.75 g

(Note: The tables are all for the mass contained in 1 L of medium.)

2.1.2. Test soil

The red clay used in this test was sourced from Yan Shan District, Guilin City, Guangxi Zhuang Autonomous Region. It was collected at a depth of 3–5 m and exhibited a brownish-red color. Indoor geotechnical tests were conducted on the soil according to the Standard for Geotechnical Test Methods (People's Republic of China Ministry of Housing and Urban-Rural Development, 2019). The basic physical properties of the test soil are listed in Table 2.

Table 2
Basic physical indicators of Guilin red clay.

Optimum moisture content ω(%)	Maximum dry density ρ_d (g/cm^3)	Specific gravity G_S	Liquid limit W_L (%)	Plastic limit W_P(%)	Plasticity Index I_P
30.00	1.51	2.73	57.95	31.22	26.73

2.1.3. Sources of pollution and curing materials

Zinc nitrate hexahydrate was selected as the heavy metal contaminant, with its composition shown in Table 3. Nitrate has good solubility and can be quickly dissolved in distilled water, with negligible interference with the hydration reaction (Qian et al., 2017; Cuisinier et al., 2011).

Table 3
Table of technical conditions for zinc nitrate hexahydrate ($Zn(NO_3)_2{\cdot}6H_2O$) (analytical purity).

Chemical compound	Content
$Zn(NO_3)_2{\cdot}6H_2O$	≥ 99.0%
pH	≥ 3.5
Watery dissolved substance	0.005%
Cl^-	0.001%
SO_4^{2-}	0.002%
Fe^{3+}	0.0003%
Pb^{2+}	0.005%
$(NH_4)_2S$	0.10%

(Note: pH was determined at a solubility of 50 g/L and a temperature of 25 ˚C)

Activated MgO, provided by Xilong Science Co. Ltd., is a white powder under normal conditions. This high-activity MgO has a content of 98.5% and a surface area of 57.94 m^2/g, as determined by NOVA1200e model instrument analysis. Its basic physical properties are shown in Table 4.

Table 4
Basic physical properties of activated MgO.

MgO content (%)	pH	Solubility	Specific surface
98.5	10.3	2.72	57.94

2.2. Test programme and specimen preparation

2.2.1. Test programme

Preliminary on-site investigations in Guilin City revealed that the Zn^{2+} pollution concentration was approximately 460 μg/g. Given the residential nature and limited scope of the investigation area, we opted for a minimum pollution concentration of 500 μg/g for the experiment, equivalent to 0.05% (Wang et al., 2022b). Since China has yet to establish zinc pollution risk standards for construction land soil, municipalities such as Beijing and Shenzhen have set the screening and control values for zinc in secondary land use at 10,000 μg/g. Below this threshold, no risk assessment is required, and the land can be directly redeveloped for its intended use. According to the results of investigations into heavy metal content in soil from a lead-zinc mining area in Guangxi, the zinc content in surface soil was found to reach 3300 μg/g (Qin, et al., 2013). Hence, we selected 10,000 μg/g (1%) as the maximum pollution concentration for the experiment. The final design incorporated pollution concentrations of 0.05%, 0.1%, 0.5%, and 1%. Based on in-situ solidification experiments, the selected dosages of activated MgO were 1%, 2%, 5%, and 10%. The experiments were conducted at or near the maximum dry density of 1.51 g/cm^3 , with dry densities of 1.35 g/cm^3 , 1.40 g/cm^3 , 1.45 g/cm^3 , and 1.50 g/cm^3 . Both the heavy metal zinc pollution concentration and the dosage of activated MgO were expressed as percentages of the dry soil mass. For the experiments, 64 specimens were prepared for unconfined compressive strength tests and direct shear tests, including parallel specimens. Direct shear tests were conducted only for the activated MgO dosage at 2%, and the experimental data were based on the average of three parallel specimens. The mixing ratios for the experiments are shown in Table 5.

Table 5
Test program.

Influencing factors	Zinc ion concentration(%)	Dry density ρ_d (g/cm^3)	MgO doping(%)
Quantity contained	0.05	1.35	1
	0.1	1.4	2
	0.5	1.45	5
	1	1.5	10

2.2.2. Microbiological culture

The kraft paper, rubber stoppers, conical flasks, and beakers containing liquid medium were autoclaved at 120 °C for 30 min. Upon removal, they were cooled on an ultra-clean bench. Once they reached room temperature, the bacterial solution stored in the refrigerator was retrieved and heated in a water bath until it reached a liquid state. Subsequently, the bacterial solution was carefully poured into a conical flask containing approximately 200 mL of liquid medium on an ultra-clean bench. The flask was then sealed with a rubber stopper and covered with kraft paper before being placed in a constant temperature shaker set at 30 °C with a rotational speed of 180 r/min for 48 h.

The spectrophotometer was switched on 30 min in advance to allow it to warm up and calibrated to measure absorbance at a wavelength of 600 nm (OD_{600}). To ensure precision and eliminate the influence of distilled water, the OD_{600} of distilled water was measured and set to zero. Subsequently, the bacterial solution incubated for 48 h in the constant temperature shaker was retrieved and placed on the ultra-clean bench. Using a pipette gun, 3 mL of the bacterial solution was transferred into a cuvette, which was then inserted into the spectrophotometer for OD_{600} measurement. An inorganic salt solution (as per Table 6) was selected for dilution to achieve an OD_{600} value of 1.2. The prepared bacterial and gelling solutions were then stored on the ultra-clean bench for subsequent use (Fig. 1A–B).

Table 6
Inorganic salt composition.

Name	Content
KH_2PO_4	0.5 g/L
Trace element	1.0 mL/L
$C_3H_5NaO_3$	3.36 g/L
K_2HPO_4	0.5 g/L
$(NH4)_2SO_4$	2.5 g/L
Na_2SO_4	1.0 g/L
$CaCl_2$	0.1 g/L
$MgSO_4$	1.0 g/L

2.2.3. Specimen preparation

The soil designated for testing underwent drying in an oven at 60 °C for 72 h to prevent excessive temperatures from affecting its bound water content. This method ensured the preservation of the soil's bound water content. Following drying, the soil was meticulously sieved through a standard 2 mm sieve. The precise amount of distilled water was measured. Thorough stirring with a glass rod ensured complete dissolution, resulting in the formation of a Zn^{2+} solution. Subsequently, the soil was placed in a preservation bag for 7 days to facilitate passivation. This process promoted equilibrium between Zn^{2+} ions and the soil particles. Finally, the prepared zinc-contaminated soil underwent another round of drying in an oven at 60 °C for 72 h.

Initially, the prepared zinc-contaminated soil was mixed with the predetermined quantity of activated MgO to ensure uniform distribution. Following this step, a specific volume of bacterial liquid and reaction fluid was measured based on achieving the optimal 30% water content. The bacterial liquid was then sprayed onto the contaminated soil, facilitating thorough mixing with the soil particles. Subsequently, the reaction fluid was added in the same manner to ensure complete reaction and homogeneity of the soil sample.

2.3. Test methods and instruments

2.3.1. Unconfined compressive strength

The contaminated soil, blended with bacterial and reaction fluid, was then weighed to match the specified dry density for the test. Following this, a standard triaxial specimen with a diameter of 39.1 mm and a height of 80 mm was meticulously prepared using the static compaction method according to the "Standard for Geotechnical Test Methods." (People's Republic of China Ministry of Housing and Urban-Rural Development, 2019). Subsequently, the unconfined compressive strength test was conducted after a 7-day curing period in a constant temperature and humidity box ((25 ± 2) °C, humidity 98% ± 2%).

2.3.2. Direct shear test

The contaminated soil was thoroughly mixed with the bacterial and reaction solutions, and the resulting mixture was weighed to prepare soil samples for the specified dry density. According to the Standard for Geotechnical Test Methods (People's Republic of China Ministry of Housing and Urban-Rural Development, 2019), remolded ring knife specimens with a diameter of 61.8 mm and a height of 20 mm were meticulously fabricated using static compaction. Following a 7-day curing period in a constant temperature and humidity chamber (maintained at (25 ± 2) °C with a humidity of 98% ± 2%), the direct shear test was conducted.

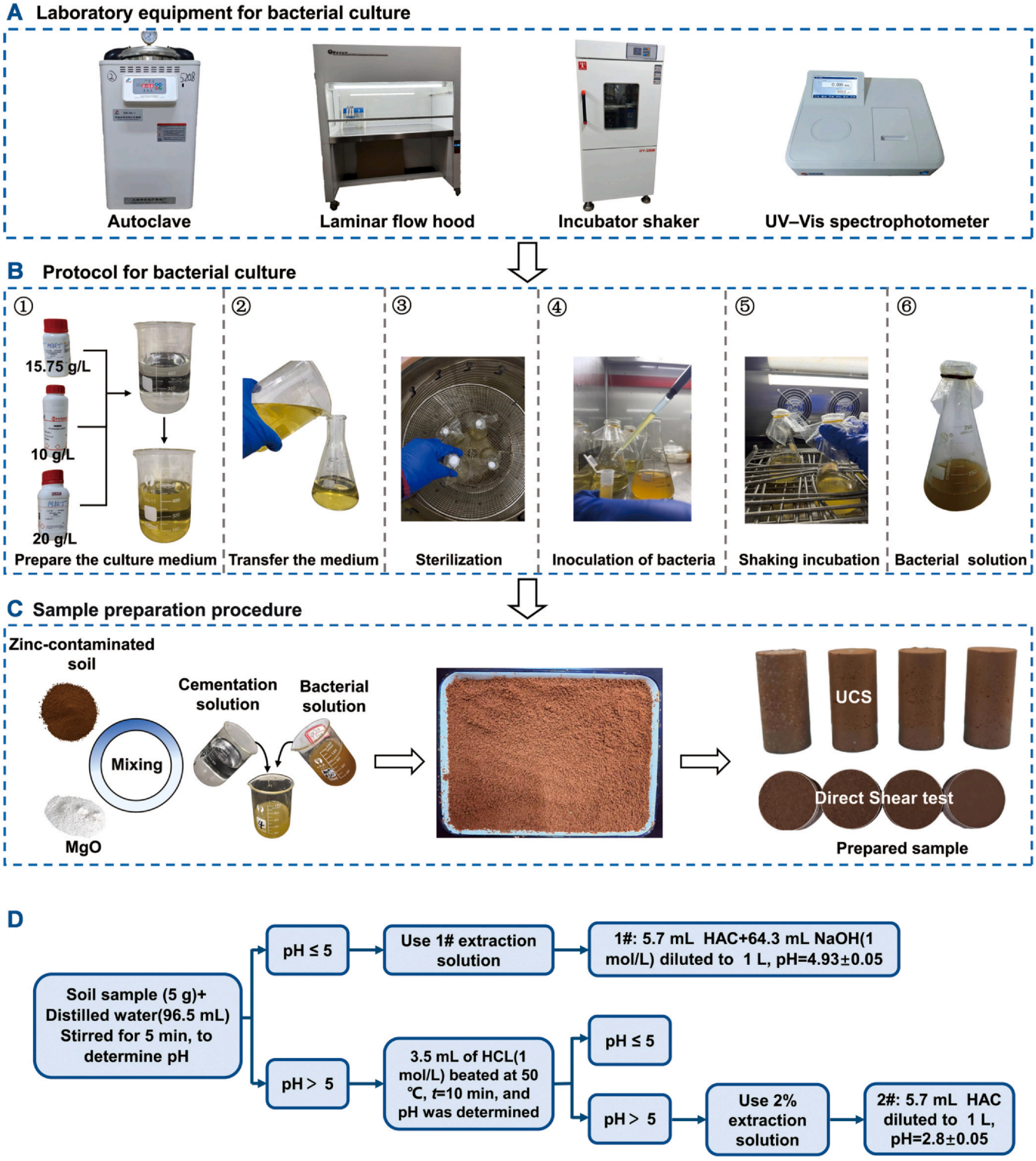

Fig. 1. Test procedure and test apparatus diagram: (**A**) Laboratory equipment for bacterial culture; (**B**) Protocol for bacterial culture; (**C**) Sample preparation procedure; (**D**) Toxicity characteristic leaching procedure flow chart.

The instrument used for the test was the ZJ-type strain-controlled quadruple straight shear apparatus manufactured by Nanjing Soil Instrument Factory, specifically designed for conducting rapid shear tests. The shear tests were performed at a rate of 0.8 mm/min under vertical pressures of 100 kPa, 200 kPa, 300 kPa, and 400 kPa. The shearing process was stopped upon reaching a shear displacement of 6 mm.

According to the formula: $\tau_f = c + \sigma \tan \varphi$ to find the shear strength index c and φ.

Where τ_f shear strength, kPa;
σ - total stress, kPa;
c - cohesion of soil, kPa;
φ - the angle of internal friction of soil(°).

2.3.3. Toxicity characteristic leaching procedure

Ten sets of soil samples, which had previously undergone the unconfined compressive strength test, were selected for further analysis.

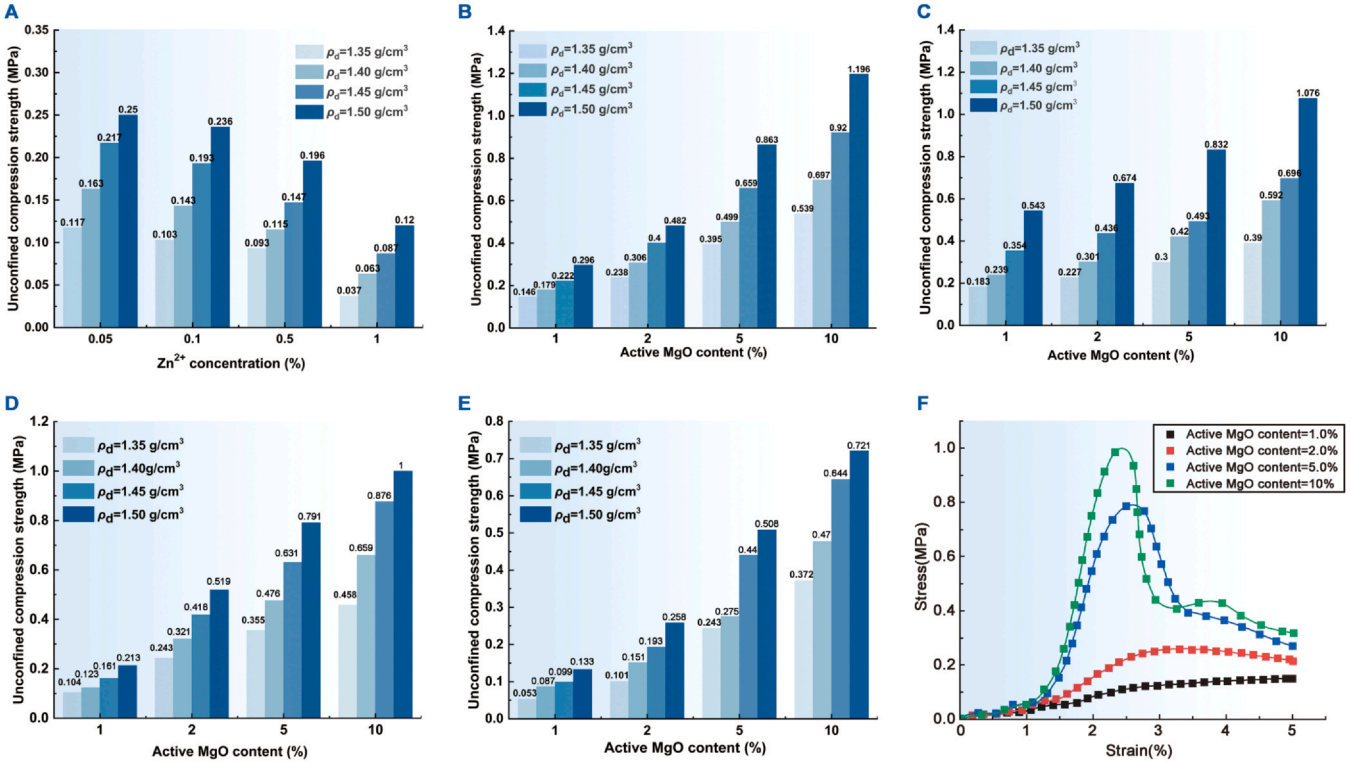

Fig. 2. Plot of peak unconfined compressive strength: (**A**) Zn^{2+} Concentration = 0%; (**B**) Zn^{2+} Concentration = 0.05%; (**C**) Zn^{2+} Concentration = 0.1%; (**D**) Zn^{2+} Concentration = 0.5%; (**E**) Zn^{2+} Concentration = 1.0%; (**F**) Stress-strain diagram for Zn^{2+} = 5%, dry density 1.5 g/cm^3.

To mitigate the potential interference of Pasteurised Spore Octococcus and other bioactive substances on the results of the toxic leaching test, the soil samples were dried at 105 °C and then sieved through a 1 mm sieve. The resulting sieved soil samples were then used to prepare the leachate for the test. This study follows the relevant regulations outlined in the United States Toxic Toxicity Characteristic Leaching Procedure. (Epa, 1992) and the U.S. Method 1311 Toxicity Characteristic Leaching Procedure (TCLP) test, utilizing leaching agent 1#. The objective of the test was to ascertain the mobility of Zn^{2+} and simulate the leaching process of zinc contamination from solid waste in the presence of landfill leachate following its disposal in a sanitary landfill. Within the scope of this study, a toxicity characteristic leaching procedure was performed to validate the stability of MICP synergistically activated MgO-cured zinc ions and to explore the mechanism of MICP synergistically activated MgO curing. The flow of the toxic leaching test is shown in Fig. 1D.

3. Results and discussion

3.1. Unconfined compressive strength test

The variation in unconfined compressive strength test results under different activated MgO doping levels, Zn^{2+} concentrations, and dry densities is illustrated in Fig. 2.

As shown in Fig. 2A, demonstrating the unconsolidated zinc-contaminated soil, the unconfined compressive strength gradually decreases with increasing zinc ion concentration, reaching a minimum of 0.037 MPa when the zinc ion concentration is 1%. Zinc ions significantly compromised the integrity of the soil structure and diminished the interparticle interactions, adversely impacting the construction quality of the project. Fig. 2 illustrates that the mechanical strength of zinc-contaminated soil stabilized through MICP combined with activated MgO has markedly increased, indicating that this method can effectively enhance the properties of zinc-contaminated soil.

Under identical Zn^{2+} concentrations, the unconfined compressive strength increases with increasing dry density, achieving values of 1.196 MPa, 1.076 MPa, 1.00 MPa, and 0.721 MPa at a dry density of 1.50 g/cm^3 with an activated MgO content of 10%. The unconfined compressive strength peaks at a dry density of 1.5 g/cm^3. This phenomenon can be attributed to the fact that higher dry density results in a more compact soil matrix, reduced pore size, and increased interparticle contact area. In engineering practice, higher dry density leads to lower compressibility and is more favourable for engineering construction.

The unconfined compressive strength progressively increases with the increase of activated MgO doping. The unconfined compressive strength of specimens doped with 10% activated MgO exhibited an increase by a factor of 1.98 to 7.89 compared to those doped with 1% activated MgO and microbially cured. It has been observed that with increasing activated MgO doping, the stress-strain curve exhibits increased brittleness, with the curve progressively shifting to the left as depicted in Fig. 2F. Activated MgO reacts with water to form the gelling substance $Mg(OH)_2$. As more activated MgO is incorporated, a greater amount of cementing material is produced, thereby enhancing the curing effect. Activated MgO reacts with water to form the gelling substance $Mg(OH)_2$. As more activated MgO is incorporated, a greater amount of cementing material is produced, thereby enhancing the curing effect (Huang et al., 2022). The curing effect of activated MgO on Zn^{2+}-contaminated soils was notably significant, markedly increasing the compressive strength. Additionally, the impact of activated MgO on Zn^{2+} during toxic leaching was substantial (details on toxic leaching are provided later).

The unconfined compressive strength of the specimens exhibited a gradual decline with increasing Zn^{2+} concentration. It decreased from 0.863 MPa to 0.508 MPa when the dry density was 1.50 g/cm^3 and the activated MgO doping was at 5%. Increasing Zn^{2+} concentration reduces the soil's dry density, leading to a higher pore ratio, consequently diminishing the unconfined compressive strength of the soil. It was observed that an increase in the unconfined compressive strength of the soil occurred when the Zn^{2+} concentration rose from 0.05% to 0.1%

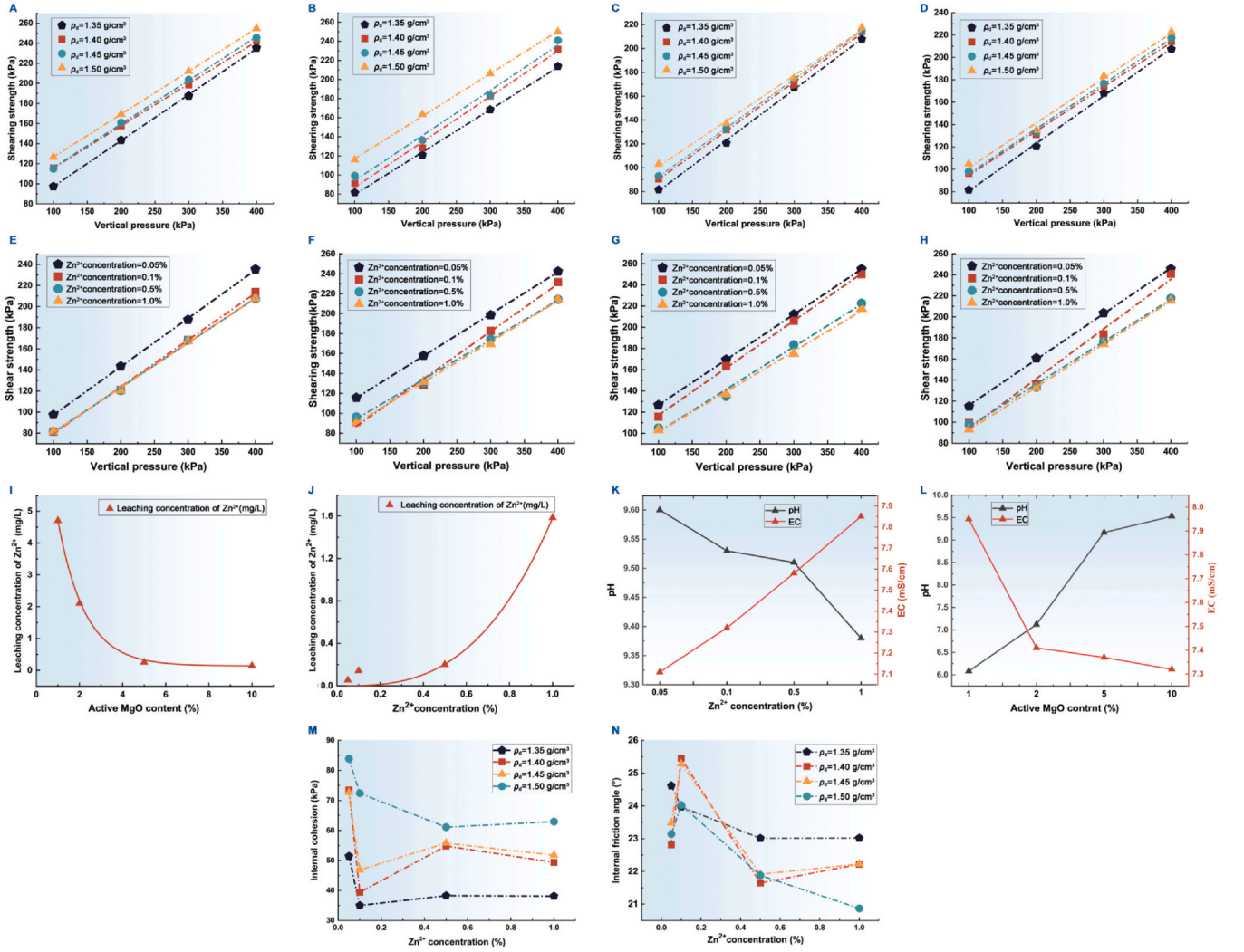

Fig. 3. MICP-activated MgO shear strength: (**A–D**) Shear strength of MICP-activated MgO cured zinc contaminated soil at different zinc ion concentrations(Zn^{2+} concentration 0.05% , 0.1%, 0.5%, 1.0%); (**E–H**) Shear strength of MICP-activated MgO cured zinc contaminated soil at different dry densities (Dry density 1.35, 1.4, 1.45, 1.5 g/cm^3); Toxicity characteristic leaching procedure: (**I**) Different active MgO dosage, (**J**) Different zinc ion concentrations, (**K**) Ph, EC: Different zinc ion concentrations, (**L**) Ph, EC: different active MgO dosage; Changes with zinc ions at different dry densities: (**M**) Cohesion, (**N**) Angle of internal friction.

with 1% activated MgO doping, along with a marginal increment and no change in the unconfined compressive strength at 2% activated MgO. This phenomenon arises from the fact that the trace amount of Zn^{2+} promotes the growth of Bartonella lactococcus, consequently enhancing the efficacy of MICP and promoting the production of increased zinc carbonate and calcium carbonate precipitates to occupy the pores. This aligns with the discovery by Kim et al. (2021), who observed that a minor quantity of Zn^{2+} stimulates bacterial growth, whereas an excess amount exerts a toxic influence, thereby impeding the efficacy of MICP.

3.2. Direct shear test

This study aims to analyze the effect of Zn^{2+} concentration and dry density on shear strength. The objective is to reduce the water absorption of activated MgO, which impacts bacterial activity. Therefore, this section focuses on examining the shear strength index in direct shear tests when the activated MgO content is 2%.

Under identical Zn^{2+} concentrations, the shear strength exhibited a complex trend across various dry densities due to the influence of four different vertical pressures (Fig. 3A–D).

It was observed that the shear strength increased with rising dry density under identical Zn^{2+} contamination concentrations. Under a vertical pressure of 100 kPa, the shear strength of the specimens exhibited greater variability with increasing dry density, demonstrating a maximum increase of 41.91%. Under a vertical pressure of 400 kPa, the variation in shear strength of the specimens with increasing dry density was reduced, with a maximum increase of 16.92% and a minimum increase of only 4.72%. This phenomenon arises from the fact that lower vertical pressure exerts a diminished impact on the internal pores of the specimen. In specimens with low dry density, the spacing between soil particles is substantial, resulting in numerous internal pores. Under higher vertical pressure, these low dry-density specimens undergo further compaction, reducing internal pores and enhancing interparticle friction. Conversely, specimens with high dry density exhibit fewer internal pores, thus experiencing minimal influence from vertical pressure on internal porosity, consequently diminishing the magnitude of the increase.

At the same dry density, the shear strength at different Zn^{2+} concentrations exhibited a complex trend influenced by four vertical pressures (Fig. 3E–H).

It was observed that the shear strength gradually decreased with increasing Zn^{2+} contamination concentration at a constant dry density. Specifically, the shear strength of red clay decreased by 37.22 kPa as the concentration of Zn^{2+} increased, under a dry density of 1.50 g/cm^3 and a vertical pressure of 400 kPa. On average, a decrease of 27.14 kPa was noted in individual specimens as the concentration of Zn^{2+}

increased. This can be attributed to the structural damage of the red clay caused by Zn^{2+}, with higher concentrations leading to more severe destruction of the red clay. Li Jiaming's experimental study further demonstrated that the increase in Zn^{2+} doping results in a gradual transition of red clay soil from a compact to a loose state. This transition is accompanied by reduced structural integrity, increased pore cracks, and diminished cementation (Li et al., 2021). When treated with 2% activated MgO, only a small portion of the Zn^{2+} contamination was mitigated. Additionally, at the macroscopic level, it was observed that specimens with lower levels of Zn^{2+} contamination exhibited bacterial traces in the presence of MIC, which internally generated white calcium carbonate. This process enhanced shear strength and aided in the remediation of Zn^{2+} contaminated soils. Conversely, in specimens with higher levels of Zn^{2+} contamination, minimal bacteria were present on the surface, and the internal production of white calcium carbonate was substantially diminished. This indicates that the elevated Zn^{2+} concentration adversely impacted bacterial metabolism.

Among samples with the same contamination concentration, a dry density of 1.50 g/cm^3 exhibits the highest shear strength indicator, implying that shear strength increases with higher dry densities. As illustrated in Fig. 3M, the cohesion of red clay treated with MICP-co-activated MgO decreased with increasing pollution concentration at constant dry densities. The decrease was notably pronounced when the Zn^{2+} concentration increased from 0.05% to 0.1%. Specifically, at dry densities of 1.50 g/cm^3, 1.45 g/cm^3, 1.40 g/cm^3, and 1.35 g/cm^3, the cohesion decreased by 13.70%, 35.56%, 46.34%, and 31.91%, respectively. This phenomenon arises from the alteration of the structural properties of soil particles induced by Zn^{2+}, leading to a reduction in the bonding between red clay particles and a decrease in the strength of inter-particle connections. As the concentration of Zn^{2+} increases, the internal resistance between soil particles diminishes, resulting in a decrease in cohesive force. As the Zn^{2+} concentration continued to rise, the dry densities of 1.45 g/cm^3, 1.40 g/cm^3, and 1.35 g/cm^3 exhibited a minor initial increase followed by a slight decrease. This could be attributed to a subsequent rise in Zn^{2+} concentration, wherein Zn^{2+} facilitates the generation of new minerals. Additionally, Zn^{2+} reacts with carbonate to form zinc carbonate, thereby impeding the decline in cohesion or even leading to a minor increase. In summary, Zn^{2+} causes the soil to fail to densify, reducing friction between soil particles, as well as between soil particles and activated MgO and calcium carbonate, leading to reduced cohesion.

Examination of Fig. 3N reveals a consistent decline in cohesion with increasing Zn^{2+} concentration at a dry density of 1.35 g/cm^3, implying that Zn^{2+} adversely affected the structural integrity of the soil, leading to a reduction in inter-particle friction. At low dry densities, the soil exhibited internal porosity, with microbially-induced production of calcium carbonate filling the pores. At dry densities of 1.40 g/cm^3, 1.45 g/cm^3, and 1.50 g/cm^3, the internal friction angle initially increases before decreasing and eventually stabilizing. This phenomenon arises from the rhombohedral shape of calcium carbonate crystals produced by microorganisms, which enhances intergranular interlocking. Furthermore, MICP collaborates with activated MgO to solidify Zn^{2+}. The resulting calcium carbonate and magnesium hydroxide cementing substances fill particle pores and adsorb Zn^{2+}, leading to a temporary increase when the Zn^{2+} concentration reaches 0.1%. With increasing Zn^{2+} contamination concentration, the viscosity of the red clay markedly increases. The proportion of large particles rises, leading to increased aggregation distance and decreased contact area, resulting in diminished friction at particle contact points. Moreover, the growth and development of Bacillus pasteurii are hindered. The minerals produced are inadequate to withstand sliding between particles, leading to a notable decrease in the internal friction angle.

3.3. Toxicity characteristic leaching procedure

The test was commissioned to Thermo Fisher Scientific Ltd. for the toxicity leaching assay using an inductively coupled plasma emission spectrometer model iCAP7600.

Fig. 3I illustrates the variation in Zn^{2+} leaching concentration during the MICP synergistic activated MgO curing process of contaminated red clay with activated MgO doping at a Zn^{2+} concentration of 0.1%. Observations from Fig. 3I reveal a pronounced decrease in Zn^{2+} leaching concentration with increasing activated MgO doping. At an activated MgO doping level of 10%, the leaching concentration of Zn^{2+} was only 0.1414 mg/L. This indicates that MICP synergistic activated MgO has a good curing and stabilizing effect on Zn^{2+}. Microorganisms produce urease to catalyze the decomposition of urea, which reacts with calcium ions in $CaCl_2$ to generate calcium carbonate, thereby curing Zn^{2+} during this process. A small amount of the generated calcium carbonate wraps around Zn^{2+}, and some carbonate ions react with Zn^{2+} to form relatively stable zinc carbonate. Additionally, activated MgO possesses the capability to remediate contaminated soil due to its large specific surface area and physical adsorption properties. Hence, activated MgO can adsorb Zn^{2+} and inhibit its leaching. The change in activated MgO doping follows a curve, as indicated by fitting Eq. 1.

$$L_{Zn} = 10.631 \times e^{\left(-\frac{C_M}{1.189}\right)} + 0.119 \quad (R^2 = 0.999) \tag{1}$$

Where L_{Zn} is Zn^{2+} leaching concentration (mg/L); C_M is activated MgO doping (%).

Fig. 3J illustrates the variation in Zn^{2+} leaching concentration as a function of Zn^{2+} concentration in MICP-enhanced activated MgO-treated contaminated red clay, with an activated MgO doping level of 10%. It is evident from Fig. 3J that as the Zn^{2+} concentration increases, the Zn^{2+} leaching concentration also rises, reaching 0.054 mg/L at a Zn^{2+} concentration of 0.05%. At a Zn^{2+} concentration of 1%, the leaching concentration of Zn^{2+} measures 1.584 mg/L, remaining below the prescribed benchmarks and restrictions delineated by the "Groundwater Quality Standard" (GB/T 14848–2017). This underscores its potential efficacy in ameliorating conditions through the synergistic activity of MICP, particularly when facilitated by MgO. Nevertheless, the leaching concentration of Zn^{2+} is notably influenced by the pollution concentration, exhibiting a relationship that can be effectively modeled by an exponential function, as demonstrated by fitting Eq. 2.

$$L_{Zn} = 1.584 \times Q_{Zn}^{2.954} \quad (R^2 = 0.986) \tag{2}$$

In Fig. 3K, it can be seen that as the activated MgO content increases, the pH of the system progressively rises. Analytical results indicate that the synergy between MICP and activated MgO reacts with heavy metal ions in the soil, leading to the formation of heavy metal carbonate precipitates. A higher pH in the leachate enhances the solidifying agent's resistance to erosion. As a result, the leachate's capacity to desorb heavy metals from the contaminated soil diminishes, leading to a reduced concentration of heavy metal ions in the leachate. Conversely, as the Zn^{2+} concentration increases, the pH gradually declines, which enhances the leachate's ability to desorb heavy metals from the contaminated soil, resulting in a higher concentration of heavy metal ions in the leachate.

In Fig.3L, it can be seen that as the activated MgO content increases, the electrical conductivity (EC) decreases. This reduction occurs because MICP, in synergy with activated MgO, immobilizes Zn^{2+} in the soil, thereby lowering the Zn^{2+} concentration in the leachate and reducing the number of conductive ions in the solution. As the Zn^{2+} concentration rises, the EC of the leachate significantly increases. This phenomenon is attributed to the presence of ions such as Mg^{2+}, Zn^{2+}, CO_3^{2-}, H^+, and NH_4^+ in the leachate, making it a strong electrolyte. The gradual increase in the content of conductive cations in the solution indicates that higher Zn^{2+} concentrations enhance the leachate's conductivity.

3.4. Mechanistic analysis of remediation of contaminated soil by MICP synergistic activated MgO solidification

(1) Activated MgO, being alkaline, reacts with water to form $Mg(OH)_2$, which has low solubility and produces flocs and precipitates. These

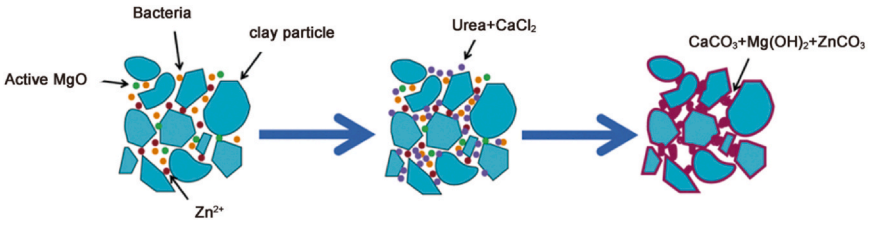

Fig. 4. Diagram of the MICP reaction process.

flocs and precipitates can encapsulate Zn^{2+}, thereby reducing its leaching concentration, while also acting as a cementing agent.

(2) Activated MgO creates an alkaline environment conducive to the proliferation of Sporosarcina pasteurii. During the MICP curing process, the reactive MgO becomes a porous structure that can provide nucleation sites for calcium carbonate generation. Consequently, the calcium carbonate precipitated serves as a cementing agent, integrating with the soil matrix rather than forming discrete, unbonded crystals within the pore spaces. The resultant cementitious material generated during the MICP process cohesively binds the loose soil particles, occludes the soil's internal porosity, and augments its dry density, thereby markedly enhancing soil strength and mitigating the leaching potential of Zn^{2+}.

Microbially Induced Carbonate Precipitation (MICP) process: Sporosarcina pasteurii produces urease, which catalyzes the hydrolysis of urea to generate NH_4^+ and CO_3^{2-} ions. CO_3^{2-} ions react with Ca^{2+} ions in $CaCl_2$ to precipitate $CaCO_3$. MgO reacts with H_2O to generate $Mg(OH)_2$, where Mg^{2+} reacts with CO_3^{2-} to produce $MgCO_3$ precipitation. The Zn^{2+} and CO_3^{2-} in the contaminant zinc nitrate hexahydrate reacted to form $ZnCO_3$ precipitate, thereby better fixing the Zn^{2+} and reducing leaching. The reaction process is shown in Fig. 4. The chemical formula of the reaction is as follows:

$$CO(NH_2)_2 + 2H_2O \rightarrow 2NH_4^+ + CO_3^{2-} \quad (3)$$

$$MgO + H_2O \rightarrow Mg(OH)_2 \quad (4)$$

$$Mg^{2+} + CO_3^{2-} \rightarrow MgCO_3\downarrow \quad (5)$$

$$Ca^{2+} + CO_3^{2-} \rightarrow CaCO_3\downarrow \quad (6)$$

$$Zn^{2+} + CO_3^{2-} \rightarrow ZnCO_3\downarrow \quad (7)$$

$$Mg^{2+} + Ca^{2+} + 2CO_3^{2-} \rightarrow MgCa(CO_3)_2\downarrow \quad (8)$$

4. Conclusion

In this paper, the influencing factors and mechanisms of MICP synergistic activated MgO curing of zinc-contaminated red clay were investigated indoors. The effects of each influencing factor on MICP synergistic activated MgO curing of zinc-contaminated red clay were analyzed by varying the dry density, Zn^{2+} concentration, and activated MgO doping during the test. Various laws were identified, and the following conclusions were drawn:

(1) MICP synergized with activated MgO can significantly enhance soil strength. At a specific Zn^{2+} concentration, activated MgO can enhance the unconfined compressive strength by 1.98 to 7.89 times. Increasing Zn^{2+} concentration generally decreases the unconfined compressive strength of the soil. However, at low Zn^{2+} concentrations, it enhances MICP effectiveness and boosts calcium carbonate production, which fills particle pores and cement soil particles, thereby increasing the soil's unconfined compressive strength. An increase in dry density leads to denser soil particles and smaller pores, which favors an increase in the soil's unconfined compressive strength.

(2) With a specific amount of activated MgO doping, a Zn^{2+} concentration of 0.05%, and a dry density of 1.50 g/cm^3, the shear strength reaches its maximum value. Zn^{2+} disrupts the cementation of soil particles, resulting in larger inter-particle pore spaces. This dispersion of the soil body consequently reduces its shear strength.

(3) MICP synergistic with activated MgO can effectively immobilize zinc in red clay. With 10% activated MgO doping, the Zn^{2+} leaching concentration reaches a minimum of only 0.1414 mg/L. The Zn^{2+} concentration significantly impacts the leaching rate, with a concentration of 0.054 mg/L observed at a Zn^{2+} concentration of 0.05%.

(4) The mechanism by which MICP synergizes with activated MgO to enhance the curing of zinc-contaminated red clay is as follows: activated MgO, being alkaline and possessing a large specific surface area, effectively adsorbs Zn^{2+}. Additionally, activated MgO provides nucleation sites for calcium carbonate formation. MICP technology, through Sporosarcina pasteurii, produces urease, which catalyzes the decomposition of urea to generate CO_3^{2-}. This CO_3^{2-} reacts with Ca^{2+} to form calcium carbonate precipitates. The calcium carbonate adsorbs and encapsulates Zn^{2+}, while some Zn^{2+} reacts with CO_3^{2-} to form zinc carbonate precipitates, thereby enhancing Zn^{2+} immobilization.

Funding

Project "Research on remediation of typical heavy metal contaminated soil in Henan Province based on EICP technology". (25200810005) supported by Henan Science and Technology R&D Program Joint Fund. Project "Ion migration and solidification repair mechanism of heavy metal contaminated soil in karst area" (No.KDL & Guangxi202303) supported by Guangxi Key Science and Technology Innovation Base on Karst Dynamics. Project Evolution law and mechanism of macro and micro characteristics of activated magnesium oxide microbial synergistic solidification of heavy metal contaminated soil" (No. 42262030) supported by the National Natural Science Foundation of China. Project "Research on mechanical properties of fiber-microbe synergistic curing of calcareous sand". (Guikeyan 2023-XT-02) supported by the open subject of Guangxi Key Laboratory of Geotechnical Mechanics and Engineering.

CRediT authorship contribution statement

Yu Song: Investigation, Funding acquisition. **Wei Liu:** Writing – review & editing. **Qiaqi Li:** Funding acquisition, Conceptualization. **Yuling Chen:** Visualization. **Jichun Cheng:** Project administration. **Jianwei Zhang:** Software. **Junjie Zheng:** Software, Methodology.

Data availability

Not applicable.

Declaration of Competing Interest

The authors declare that they have no known competing financial interests or personal relationships that could have appeared to influence the work reported in this paper.

References

Cuisinier, O., Le Borgne, T., Deneele, D., & Masrouri, F. (2011). Quantification of the effects of nitrates, phosphates and chlorides on soil stabilization with lime and cement. *Engineering Geology, 117*(3–4), 229–235. https://doi.org/10.1016/j.enggeo.2010.11.002

Dong, Y., Gao, Z., Di, J., Wang, D., Yang, Z., Wang, Y., & Li, K. (2023). Experimental study on solidification and remediation of lead–zinc tailings based on microbially induced calcium carbonate precipitation (MICP). *Construction and Building Materials, 369*, 130611. https://doi.org/10.1016/j.conbuildmat.2023.130611

Epa, U. S. (1992). M-1311, test method 1311-toxicity characteristic leaching procedure. *EPA-SW-846 Online*.

Hu, Q. Z., Huo, W. Y., Ma, Q., et al. (2023). Research on mechanics and water stability of fiber reinforced loess combined with MICP +248. *Yangtze River, 54*(08), 227–232. https://doi.org/10.16232/j.cnki.1001-4179.2023.08.032

Huang, T., Fang, X. W., Zhang, W., et al. (2022). Experimental study on solidified loess by microbes and reactive magnesium oxide +3316. *Rock and Soil Mechanics, 41*(10), 3300–3306. https://doi.org/10.16285/j.rsm.2020.0151

Ji, G. S., Huan, C. C., Zeng, Y., et al. (2024). Microbiologically induced calcite precipitation (MICP) in situ remediated heavy metal contamination in sludge nutrient soil. *Journal of Hazardous Materials, 473*. https://doi.org/10.1016/j.jhazmat.2024.134600

Jiang, Z., Peng, J., Xu, P. X., et al. (2022). High strength test study on coral sand re-inforced by microbe High strength test study on coral sand reinforced by microbe and fiber. *Journal of Civil and Environmental Engineering,* 2096–6717.

Kim, Y., Kwon, S., & Roh, Y. (2021). Effect of divalent cations (Cu, Zn, Pb, Cd, and Sr) on microbially induced calcium carbonate precipitation and mineralogical properties. *Frontiers in Microbiology, 12*. https://doi.org/10.3389/fmicb.2021.646748

Li, C., Lie, T., Dong, C. H., et al. (2022). Experimental study on zinc-lead composite contaminated soil solidified/stabilized by MICP technology combined with porous silicon adsorption materials. *Rock and Soil Mechanics, 43*(02), 307–316. https://doi.org/10.16285/j.rsm.2021.1403

Li, J. M., Tang, S. B., & Chen, X. J. (2021). Analysis of the mechanical properties and mechanism of zinc ion-contaminated red clay. *Advances in Materials Science and Engineering*(1), https://doi.org/10.1155/2021/6649691

Liu, S. Y., & Li, C. (2015). Research on the effect of magnesium oxide activity on carbonation curing effect. *Journal of Geotechnical Engineering, 37*(01), 148–155. https://doi.org/10.11779/CJGE201501018

People's Republic of China ministry of housing and urban-rural development. *GB/T 50123-2019.Ministry of housing and urban-rural development of the People's Republic of China.* State Administration for Market Regulation.

Qian, X., Fang, C., Huang, M., & Achal, V. (2017). Characterization of fungal-mediated carbonate precipitation in the biomineralization of chromate and lead from an aqueous solution and soil. *Journal of Cleaner Production, 164*, 198–208. https://doi.org/10.1016/j.jclepro.2017.06.195

Qin, C. K., Yi, H., Liu, J. J., et al. (2013). Investigation and evaluation of soil heavy metal pollution in wastewater pooling depression of a lead-zinc mining area in Guangxi. *China Karst, 32*(03), 318–324.

Rajendran, S., Priya, T. A. K., Khoo, K. S., Hoang, T. K., Ng, H. S., Munawaroh, H. S. H., & Show, P. L. (2022). A critical review on various remediation approaches for heavy metal contaminants removal from contaminated soils. *Chemosphere, 287*(4), 132369. https://doi.org/10.1016/j.chemosphere.2021.132369

Shan, Y., Liang, J. L., Tong, H. W., et al. (2022). Effect of different fibers on small-strain dynamic properties of microbially induced calcite precipitation–fiber combined re-inforced calcareous sand. *Construction and Building Materials, 322*. https://doi.org/10.1016/j.conbuildmat.2022.126343

Shen, L., Wu, R. R., Xu, R. Y., et al. (2023). Bio-remediation of waters polluted by heavy metals using MICP technology:A Review. *Environmental Science & Technology, 46*(03), 9–22. https://doi.org/10.19672/j.cnki.1003-6504.2227.22.338

Song, Y., Lai, Y., Chen, Y., et al. (2026). The strength response and crack evolution of Pb^{2+} contaminated soil repaired by MICP combined with MgO under dry–wet cycle. *Water, Air, & Soil Pollution, 237*(10), 574. https://doi.org/10.1007/S11270-026-09213-W

Teng, Y., Ni, S., Wang, J., Zuo, R., & Yang, J. (2010). A geochemical survey of trace elements in agricultural and non-agricultural topsoil in Dexing area, China. *Journal of Geochemical Exploration, 104*(3), 118–127. https://doi.org/10.1016/j.gexplo.2010.01.006

Torres-Aravena, Á. E., Duarte-Nass, C., Azócar, L., Mella-Herrera, R., Rivas, M., & Jeison, D. (2018). Can microbially induced calcite precipitation (MICP) through a ureolytic pathway be successfully applied for removing heavy metals from wastewaters? *Crystals, 8*(11), 438. https://doi.org/10.3390/cryst8110438

Verma, S., Bhatt, P., Verma, A., Mudila, H., Prasher, P., & Rene, E. R. (2021). Microbial technologies for heavy metal remediation: effect of process conditions and current practices. *Clean Technologies and Environmental Policy,* 1485–1507. https://doi.org/10.1007/s10098-021-02029-8

Wang, Q. F., Chen, B. M., Li, J. Y., & Liu, X. W. (2003). Research progress in effect of urbanization on urban soil environment. *Journal of Soil and Water Conservation, 17*(04), 142–145. https://doi.org/10.13870/j.cnki.stbcxb.2003.04.039

Wang, B. K., Jia, C. Q., Wang, G. H., et al. (2022a). Study on Cementation effect of tailing sand by magnesium oxide combined with microorganism or by MICP. *Industrial. Construction, 52*(11), 79–83. https://doi.org/10.13204/j.gyjzg21022609

Wang, L. W., Rinklebe, J., Tack, F. M. G., et al. (2021). A review of green remediation strategies for heavy metal contaminated soil. *Soil Use and Management, 37*(4), 936–963. https://doi.org/10.1111/sum.12717

Wang, J. Q., Song, Y., Dong, S. S., Ding, S., Geng, Y. G., & Gao, X. T. (2022b). Triaxial experimental study of zinc contaminated red clay under different temperature conditions. *Applied Sciences, 12*(21), 10742. https://doi.org/10.3390/app122110742

Wang, R., Wan, W., & Liu, P. (2025). Experimental study on stabilization of heavy metal-contaminated soil by biochar–MICP–electrokinetics combined technology. *Sustainability, 17*(21), 9811. https://doi.org/10.3390/su17219811

Warren, L. A., Maurice, P. A., Parmar, N., & Ferris, F. G. (2001). Microbially mediated calcium carbonate precipitation: Implications for interpreting calcite precipitation and for solid-phase capture of inorganic contaminants. *Geomicrobiology Journal, 18*(1), 93–115. https://doi.org/10.1080/01490450151079833

Xu, D. M., Fu, R. B., Wang, J. X., Shi, Y. X., & Guo, X. P. (2021). Chemical stabilization remediation for heavy metals in contaminated soils on the latest decade: Available stabilizing materials and associated evaluation methods-A critical review. *Journal of Cleaner Production, 321*, Article 128730. https://doi.org/10.1016/j.jclepro.2021.128730

Xu, F., & Wang, D. (2023). Review on soil solidification and heavy metal stabilization by microbial-induced carbonate precipitation (MICP) technology. *Geomicrobiology Journal, 40*(6), 503–518. https://doi.org/10.1080/01490451.2023.2208113

Xu, Q., Wu, B., & Chai, X. (2022). In situ remediation technology for heavy metal contaminated sediment: a review. *International Journal of Environmental Research and Public Health, 19*(24), Article 16767. https://doi.org/10.3390/ijerph192416767

Zha, F. S., Chen, S. G., Kang, B., et al. (2022). Synergistic solidification of lead-contaminated soil by magnesium oxide and microorganisms. *Chemosphere, 308*(PT 2), https://doi.org/10.1016/j.chemosphere.2022.136422

Zha, F. S., Yang, Z. L., Kang, B., et al. (2024). Electrical resistivity evaluation of MICP solidified lead contaminated soil. *Environmental Earth Sciences, 83*(8), 1–13. https://doi.org/10.1007/s12665-024-11568-4